Finite Volume Analysis of the two competing-species chemotaxis models with general diffusive functions

GEORGES CHAMOUN
Faculty of Engineering (ESIB)
Saint Joseph University of Beirut
B.P 11-514 Riad El Solh, Beyrouth 1107 2050
LEBANON

Abstract: This paper aims to see how different spatial and environmental factors affect the coexistence or the exclusion of two species, while chemotaxis draws them towards a higher concentration of nutrients. For that, we analyze a robust numerical scheme applied for competitive two-species chemotaxis models with heterogeneous and potentially discontinuous diffusive coefficients. This extension is essential because diffusion can lead to discontinuities when the conductivities of the medium's components differ. In this work, we examine a generalized finite volume scheme on admissible meshes, where the line joining the circumcenters of two neighboring volumes is orthogonal to their common interface, and the discontinuities coincide with the mesh interfaces. Finite volume methods are well-suited for problems involving conservation laws and can naturally handle discontinuities, making them an ideal candidate. To achieve the convergence, we first derive the discrete problem and then we show that the discrete solution converges to a weak solution of the continuous model. Finally, many simulations were performed using Fortran software, with the introduction of a reliable computational algorithm. The efficiency of our numerical approach for finding the discrete solutions is then carefully evaluated with many test cases focusing on the heterogeneity and the discontinuity of the diffusive coefficients.

Key-Words: Lotka-Volterra Kinetics, Two-species Chemotaxis models, Discontinuous and heterogeneous coefficients, Nonlinear degenerate functions, Finite Volume method (FV).

Received: May 18, 2024. Revised: December 21, 2024. Accepted: January 16, 2025. Published: April 14, 2025.

1 Introduction

Cancer metastasis, wound healing, and immune responses are some of the important biological systems based on the chemotaxis process. Understanding this motion of the density of cells $U(x,t)$ towards a chemical stimulus $V(x,t)$ has been widely explored mathematically and numerically through variants of the Keller-Segel model, initially introduced [1] as:

$$\begin{cases} \partial_t U - \Delta U + \operatorname{div}(\Gamma_1(U)\cdot\nabla V) = 0 \\ \\ \partial_t V - \Delta V = \tilde{\alpha}U - \tilde{\beta}V \end{cases}. \quad (1)$$

The equations are parabolic partial differential equations and the positive sign of the chemotactic sensitivity Γ_1 denotes the attraction of the cells towards the chemical substrates. This system has been widely studied recently on continuous domains in [2], [3], [4], [5], [6], [7], and even on weighted networks in [8]. In this work, the tensors are reduced to the identity and we are treating the case of general isotropic functions. The anisotropic tensors and their effects cases have been studied in [9]. These isotropic models, especially for two competitive species, exhibit rich dynamics that can be applied to population interactions, tumor growth, and other biological phenomena, as in [10].

To simulate complex behaviors such as prey evasion or predator pursuit, the Lotka-Volterra competition of two species $U(x,t)$ and $W(x,t)$ was introduced as a set of ordinary differential equations (ODEs):

$$\begin{cases} \dot{U} &= \mu_1 U(1-U-\alpha_1 W) \\ \dot{W} &= \mu_2 W(1-W-\alpha_2 U). \end{cases} \quad (2)$$

The parameters μ_1 and μ_2 are the growth rates, while α_1 and α_2 denote the interaction coefficients between the species. We may have a weak competition regime and consequently a coexistence of the two species if $\alpha_1,\ \alpha_2 \in (0,1)$ or a strong competition regime in other cases of [11], [12], [13] and [14].

A significant challenge in modeling such processes arises when the medium is heterogeneous, and more specifically, when they exhibit discontinuities. This work aims to include general heterogeneous diffusive and convective coefficients, taking into account the different diffusive space properties and chemical

decay. This spatial heterogeneity requires more advanced mathematical formulations and may lead to various behaviors such as exclusion. For that, we analyze the following generalized competing two-species chemotaxis model:

$$\begin{cases} \partial_t U - \nabla \cdot \Big(q(x)\big(a(U)\nabla U - \Gamma_1(U)\nabla V\big)\Big) \\ = \mu_1 U(1 - U - \alpha_1 W), \\ \\ \partial_t W - \nabla \cdot \Big(r(x)\big(b(W)\nabla W - \Gamma_2(W)\nabla V\big)\Big) \\ = \mu_2 W(1 - W - \alpha_2 U), \\ \\ \partial_t V - \nabla \cdot (s(x)\nabla V) = -(\alpha U + \beta W)V, \end{cases} \tag{3}$$

in $\Omega \times]0, T]$ where Ω is an open bounded domain in $\mathbb{R}^d$ ($d \leq 4$) with smooth boundary $\partial\Omega$. The system is supplemented by the following boundary conditions on $\partial\Omega \times (0, T)$,

$$q(x)a(U)\nabla U \cdot \eta = 0, r(x)b(W)\nabla W \cdot \eta = 0, \tag{4}$$
$$s(x)\nabla V \cdot \eta = 0,$$

where η is the exterior unit normal to $\partial\Omega$. The initial conditions on Ω are given by,

$$U(x, 0) = U_0(x), W(x, 0) = W_0(x), \tag{5}$$
$$V(x, 0) = V_0(x)\,.$$

The details, regarding all the variables of the system (3), are provided in the Table 1.

Nonlinear and degenerate diffusive terms, detailed in [15], are denoted by $a(U)$ and $b(W)$. They approach zero as the population densities U and W are close to 0 or a normalized density 1. This threshold condition, needed to prevent overcrowding, has a clear biological interpretation was introduced in [16] and was called "volume-filling effect". Hence, we suppose initially that $\Gamma_1(0) = \Gamma_2(0) = 0$ and that the chemotactic sensitivities Γ_1 and Γ_2 vanish when $U \geq 1$ and $W \geq 1$. Next, the space heterogeneity is given through the general functions $q(x)$, $r(x)$ and $s(x)$. Furthermore, the global existence of weak solutions of the model (3) is easily guaranteed from [17], [18], [19] and [20], hence our system is well-posed.

While this study primarily focuses on the impact of heterogeneous and discontinuous diffusion coefficients on two-species chemotaxis models, future research could explore the dynamics in more complex and time-evolving environments. Incorporating feedback mechanisms, where the species influence and modify the environmental properties (e.g., nutrient depletion or enrichment), could add further realism and predictive power. These developments would be instrumental in understanding ecological systems, designing conservation strategies, and addressing challenges in multi-species bioengineering applications.

Table 1: Variables description

Variables	**Description**
U, W	The density of species 1 and 2
V	The concentration of the chemical
q, r **and** s	The anisotropic heterogeneous diffusive tensors
$a(U)$, $b(W)$	The density-dependent diffusion coefficients
$\Gamma_1(U)$, $\Gamma_2(W)$	The chemotactic sensitivity functions
μ_1, $\mu_2 > 0$	The growth rate of populations 1 and 2
α_1, $\alpha_2 > 0$	The strength of populations 1 and 2 in competition
α, $\beta > 0$	The consumption rate of chemicals by populations 1 and 2

To realistically understand the system (3), this paper focuses on the numerical study because most existing results in the literature are valid for systems with linear non-degenerate isotropic diffusion of one species and with zero logistic source terms. The finite difference and the finite element methods were used in recent papers [21], [22], [23], [24], [25] and [26]. But, the unknowns of our model (3) must be confined over $[0, 1]$, and hence the discrete maximum principle must be satisfied. Consequently, this work aims to introduce a general finite volume method to tackle the challenges of heterogeneous and discontinuous diffusion. The proposed scheme is designed to ensure that the convergence of the numerical solution towards the weak solution is maintained, even when the diffusion coefficients are discontinuous across the mesh. Finally, multiple test cases are considered to evaluate the scheme's efficiency. The accuracy and reliability of our model enhance its predictive capabilities for real-world biological systems. Hence, the

numerical implementation is notably powerful and can be easily generalized to strengthen the understanding of the multiple competing species responding to various chemical stimuli influenced by discontinuous and heterogeneous diffusive coefficients as in [27], [28], [29] and [30].

2 Setting of the problem

The assumptions given in this section, ensure that our model remains biologically realistic and mathematically well-posed. The main assumptions are as follows:

$$\text{The functions } a,\ b,\ \Gamma_1,\ \Gamma_2 \text{ belong to the set} \tag{6}$$

$$\{w \in C([0,1],\mathbb{R}^+) \text{ such that } w(0)=w(1)=0\}\,.$$

The diffusive coefficients verify:

$$q, r \text{ and } s \in L^\infty(\Omega)\,, \tag{7}$$

and there exist $\overline{q},\overline{r}$ and $\overline{s} \in \mathbb{R}_+^*$ and $\underline{q},\underline{r}$ and $\underline{s} \in \mathbb{R}_+^*$ such that a.e. $x \in \Omega, \forall \xi \in \mathbb{R}^d$,

$$\underline{q} \le q \le \overline{q},\ \underline{r} \le r \le \overline{r},\ \text{ and } \underline{s} \le s \le \overline{s} \text{ a.e. } . \tag{8}$$

Furthermore, the initial conditions are bounded as follows:

$$0 \le U_0 \le 1,\ 0 \le W_0 \le 1, V_0 \ge 0 \text{ a.e. in } \Omega \tag{9}$$

$$\text{and } V_0 \in L^\infty(\Omega)\,.$$

Definition 2.1. *A triplet* (U,W,V) *is called a* **weak solution** *of* (3)-(5) *if*

$$0 \le U(x,t) \le 1,\ 0 \le W(x,t) \le 1,\ V(x,t) \ge 0$$
$$U, W \in C_w(0,T;L^2(\Omega)),$$
$$\partial_t U, \partial_t W \in L^2(0,T;(H^1(\Omega))'),$$
$$a(U) := \int_0^U a(r)dr,\ B(W) \in L^2(0,T;H^1(\Omega))\,,$$
$$V \in L^\infty(Q_T) \cap L^2(0,T;H^1(\Omega)) \cap C(0,T;L^2(\Omega));$$
$$\partial_t V \in L^2(0,T;(H^1(\Omega))'),$$

and (U,W,V) *satisfy*

$$\int_0^T < \partial_t U, \psi_1 >_{(H^1)',H^1} dt \tag{10}$$
$$+ \iint_{Q_T} [q(x)(a(U)\nabla U - \Gamma_1(U)\nabla V)] \cdot \nabla\psi_1 \, dxdt$$
$$= \mu_1 \iint_{Q_T} U(1-U-\alpha_1 W)\psi_1 \, dxdt\,,$$

$$\int_0^T < \partial_t W, \psi_2 >_{(H^1)',H^1} dt \tag{11}$$
$$+ \iint_{Q_T} [r(x)(b(W)\nabla W - \Gamma_2(W)\nabla V)] \cdot \nabla\psi_2 \, dxdt$$
$$= \mu_2 \iint_{Q_T} W(1-W-\alpha_2 U)\psi_2 \, dxdt\,,$$

$$\int_0^T < \partial_t V, \psi_3 >_{(H^1)',H^1} dt \tag{12}$$
$$+ \iint_{Q_T} s(x)\nabla V \cdot \nabla\psi_3 \, dxdt$$
$$= -\iint_{Q_T} (\alpha U + \beta W)V\psi_3 \, dxdt\,,$$

for all ψ_1, ψ_2 and $\psi_3 \in L^2(0,T;H^1(\Omega))$, where $C_w(0,T;L^2(\Omega))$ denotes the continuous functions onto $L^2(\Omega)$ endowed with the weak topology.

3 Discrete problem

This section is dedicated to formulating the generalized finite volume scheme initially detailed in [31] and [32]. First, the spatial and temporal discretizations are described, followed by the presentation of the numerical scheme.

3.1 Discretization in space

We recall that the domain Ω is a bounded, polygonal, and connected open set with boundary $\partial\Omega$ and that it is included in $\mathbb{R}^d$ ($d=2$ or $d=3$). A mesh $\mathcal{T}_h$ of the domain Ω, as in Figure 1, consisting of open and convex polygons K known as control volumes, is said to be admissible if it satisfies the following properties:

- The closure of the union of the K's is $\bar{\Omega}$.
- The intersection between two neighboring volumes K and L is either a vertex or an edge in two dimensions (a face in three dimensions). Therefore, the $\partial K \cap \partial L$ measure is non-zero.
- There exists a family $\mathcal{P} = (x_K)_{K\in\mathcal{T}_h}$, where x_K is the center of the volume K such that $\overline{x_K x_L} \perp \sigma_{K,L}$, where $\sigma_{K,L}$ is the common interface between two neighboring control volumes. In the case of a triangulation, x_K is the center of the circumcircle of K.
- The discontinuities of q, r and s coincide with the mesh interfaces.
- The mesh size: $\tilde{h}$= sup{diam(K), $K \in \mathcal{T}_h$}.

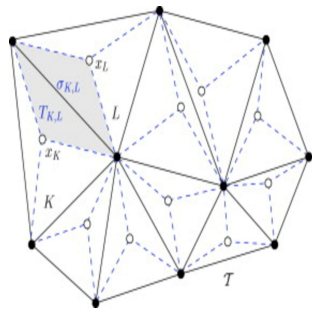

Figure 1: Admissible Space Discretization of Ω.

- $|K|$ =meas(K) represents the d-dimensional Lebesgue measure of K (the area of K in $2D$ and the volume of K in $3D$) and $|\sigma|$ is the $(d-1)$-dimensional measure of σ.
- $\mathcal{E}_{int}$ is the set of interior edges of the mesh, and $\mathcal{E}_{ext} = \{\sigma; \sigma \subset \partial\Omega\}$ is the set of boundary edges.
- $d_{K,L}$ is the Euclidean distance between x_K and x_L. If $\sigma \subset \partial\Omega$ then $d_{K,\sigma}$ is the Euclidean distance between x_K and y_σ where y_σ is the orthogonal projection- of x_K onto σ.
- $\eta_{K,L}$ is the outward normal from K that is orthogonal to $\sigma_{K,L}$; $\eta_{K,L} = -\eta_{L,K}$.
- $\tau_{K,L}$ is the transmissibility across the interface $\sigma_{K,L}$ defined as:

$$\tau_{K,L} = \frac{|\sigma_{K,L}|}{d_{K,L}}\,.$$

- $N(K) = \{L \in \mathcal{T}_h / \partial K \cap \partial L \neq \emptyset\}$ is the set of neighboring volumes of K.
- $T_{K,L}$ is the convex diamond formed by connecting the neighboring centers x_K and x_L to the vertices of the common interface $\sigma_{K,L}$. We have:

$$\Omega = \bigcup_{K\in\mathcal{T}_h} \Big(\bigcup_{L\in N(K)} \bar{T}_{K,L} \Big)\,.$$

3.2 Time discretization

The discrete unknowns are denoted as $w_K^n = w(x_K, t_n)$ for $w = U$, W or V, with $t_n = n\Delta t$ for $n \in \{0, \cdots, \tilde{N} - 1\}$.

Let $\mathcal{D}$ be an admissible discretization of $Q_T = \Omega \times [0, T]$, which is simply an admissible mesh $\mathcal{T}_h$ of Ω combined with a fixed time step $\Delta t > 0$. Therefore,

$$h = \max\{\Delta t,\ \max_{K\in\mathcal{T}_h} diam(K),\ \max_{K\in\mathcal{T}_h}\max_{L\in N(K)} d_{K,L}\}\,.$$

3.3 Associated Discrete Functions

We identify W with a piecewise constant function w_h on Ω such that $w_h|_K = W_K$, $\forall K \in \mathcal{T}_h$. Consequently, the norm in $L^2(\Omega)$ is defined as:

$$||w_h||^2_{L^2(\Omega)} = \sum_{K\in\mathcal{T}_h} |K| \big|W_K\big|^2\,,$$

and a discrete semi-norm in $H_0^1(\Omega)$ is defined as:

$$|w_h|^2_{H_0^1(\Omega)} = d \sum_{K\in\mathcal{T}_h} \sum_{L\in N(K)} \frac{|\sigma_{K,L}|}{d_{K,L}} (W_L - W_K)^2\,.$$

Next, the discrete gradient of w_h is defined as a constant over each diamond $T_{K,L}$:

$$(\nabla_h w_h)\Big|_{T_{K,L}} = \nabla_{K,L} w_h := d\frac{W_L - W_K}{d_{K,L}} \eta_{K,L}\,. \tag{13}$$

Note that the d-dimensional measure $|T_{K,L}|$is equal to $\frac{1}{d}|\sigma_{K,L}|d_{K,L}$.

3.4 Construction of the finite volume scheme

To discretize equations (3)-(5), we formally integrate both equations over each control volume K and use Stokes' theorem for the divergence integrals. Since the integral over the boundary ∂K is the sum of the integrals over the edges (or faces) of the volume K, and based on hypothesis (4), we disregard the exterior edges, as the boundary fluxes are zero. The first equation leads to:

$$\int_K \partial_t U\, dx - \sum_{L\in N(K)} \int_{\sigma_{K,L}} q(x) a(U) \nabla U \cdot \eta_{K,L}\, d\gamma(x)$$

$$- \sum_{L\in N(K)} \int_{\sigma_{K,L}} q(x) \Gamma_1(U) \nabla V \cdot \eta_{K,L}\, d\gamma(x)$$

$$= \mu_1 \int_K U(1 - U - \alpha_1 W)\, dx\,.$$

3.4.1 Diffusive Term

The calculation of the numerical diffusive flux requires approximating the values of $q(x)\nabla A(U) \cdot \eta_{K,L}$ on the interfaces $\sigma_{K,L}$. For continuous scalar diffusive functions (q, r and s) through admissible

mesh $\mathcal{T}_h$, the approximate value of the normal diffusive flux can be computed as:

$$\int_{\sigma_{K,L}} q(x)\nabla A(U)\cdot\eta_{K,L}\,d\gamma(x) \tag{14}$$

$$\approx q_{K,L}\frac{|\sigma_{K,L}|}{d_{K,L}}\big(A(U_L)-A(U_K)\big)\,,$$

where $q_{K,L} := q(\overline{x}_{K,L})$ is the approximation of $q(x)$ and $\bar{x}_{K,L}$ is the intersection point of $\sigma_{K,L}$ with the segment $[x_K, x_L]$. Consequently, the new transmissibilities are:

$$\tau_{K,L} = q_{K,L}\frac{|\sigma_{K,L}|}{d_{K,L}}\,. \tag{15}$$

To handle discontinuities of diffusive coefficients that coincide with the mesh interfaces, we introduce:

$$q_K = \frac{1}{|K|}\int_K q(x)\,dx \text{ and } q_{K,\sigma} = |q_K\eta_{K,\sigma}|\,, \tag{16}$$

where $|.|$ denotes the Euclidean norm, $q_{K,\sigma}$ is the approximation of $q(x)$ on the interface $\sigma = \sigma_{K,L}$ and $\eta_{K,\sigma}$ is the outward-pointing unit normal vector orthogonal to K.

To ensure a conservative flux, we introduce auxiliary unknown u_σ on the interfaces. These unknowns help in writing the numerical scheme but are locally eliminated to express the discrete problem only in terms of the primary unknowns $(U_K)_{K\in\mathcal{T}_h}$. Since q is continuous on both K and L, the approximation H_σ of $q(x)\nabla A(U)\cdot\eta_{K,L}$ can be calculated on each side of $\sigma_{K,L}$ using finite differences:

$$H_\sigma = q_{K,\sigma}\frac{A(U_\sigma)-A(U_K)}{d_{K,\sigma}} \text{ on } K\,,$$

$$H_\sigma = q_{L,\sigma}\frac{A(U_L)-A(U_\sigma)}{d_{L,\sigma}} \text{ on } L\,.$$

By enforcing the equality of these two approximations (conservation of the diffusive flux), we derive the following expression for $A(U_\sigma)$,

$$A(U_\sigma) = \frac{1}{\frac{q_{L,\sigma}}{d_{L,\sigma}}+\frac{q_{K,\sigma}}{d_{K,\sigma}}}\Big(A(U_L)\frac{q_{L,\sigma}}{d_{L,\sigma}} + A(U_K)\frac{q_{K,\sigma}}{d_{K,\sigma}}\Big)\,.$$

Plugging into any form of H_σ to obtain:

$$H_\sigma = \tau_\sigma(A(U_L)-A(U_K));\ \tau_\sigma = \frac{q_{K,\sigma}q_{L,\sigma}}{q_{L,\sigma}d_{K,\sigma}+q_{K,\sigma}d_{L,\sigma}}\,. \tag{17}$$

Thus, we have:

$$\int_{\sigma_{K,L}} q(x)\nabla A(U)\cdot\eta_{K,L}d\gamma \approx \tau_\sigma|\sigma_{K,L}|\big(A(U_L)-A(U_K)\big) \tag{18}$$

with the updated transmissibilities:

$$\tau^q_{K,L} = \begin{cases} q(\overline{x}_{K,L})\frac{|\sigma_{K,L}|}{d_{K,L}} & \text{if } q \text{ is continuous} \\ \tau_\sigma\,|\sigma_{K,L}| & \text{if not across interfaces}\end{cases}\,. \tag{19}$$

Similar reasoning can be applied to approximate the normal flux $q(x)\nabla V\cdot\eta_{K,L}$:

$$\delta V_{K,L} = \tau^q_{K,L}(V_L - V_K)\,.$$

Notice that we can express these transmissibilities at the interfaces by using the arithmetic mean of the approximations of the diffusive function $q(x)$ over the two adjacent triangles at the interface as follows:

$$\tau_{K,L} = \frac{|\sigma_{K,L}|}{d_{K,L}}\frac{(q_{K,\sigma}+q_{L,\sigma})}{2}\,. \tag{20}$$

However, the transmissibilities given by equation (19) yield more accurate approximate solutions.

3.4.2 Convective Term

To compute the numerical convective flux, we approximate $q(x)\Gamma_1(U)\nabla V\cdot\eta_{K,L}$ using the same numerical flux function $G(U_K, U_L, \delta V_{K,L})$ defined in [33]. The function G with arguments $(a,b,c)\in\mathbb{R}^3$ satisfies the following properties:

- $G(.,b,c)$ is increasing, $\forall\, b,c\in\mathbb{R}$ and $G(a,.,c)$ is decreasing, $\forall\, a,c\in\mathbb{R}$.
- $G(a,b,c)$=-$G(b,a,-c)$ $\forall\, a,b,c\in\mathbb{R}$; thus the flux is conservative.
- $G(a,a,c)$= $\chi(a)$c $\forall\ a,c\in\mathbb{R}$, ensuring consistency.
- There exists a constant $C>0$ such that $\forall\ a,b,c\in\mathbb{R}$, $|G(a,b,c)|\le C(|a|+|b|)|c|$.
- There exists a modulus of continuity $\omega : \mathbb{R}^+\longrightarrow\mathbb{R}^+$ such that $\forall a,b,a',b',c\in\mathbb{R}$, $|G(a,b,c)-G(a',b',c)|\le|c|w(|a-a'|+|b-b'|)$.

Remark 3.1. *An example of a numerical flux G that satisfies the above properties is by decomposing Γ_1 into its increasing part $\Gamma_1^\uparrow$ and its decreasing part $\Gamma_1^\downarrow$:*

$$\Gamma_1^\uparrow(z) := \int_0^z(\Gamma_1'(s))^+\,ds,\ \Gamma_1^\downarrow(z) := \int_0^z(\Gamma_1'(s))^-\,ds\,.$$

where,

$$s^+ = \max(s,0) \text{ and } s^- = \max(-s,0)\,.$$

Thus,

$$G(a,b,c) = c^+\big(\Gamma_1^{\uparrow}(a) + \Gamma_1^{\downarrow}(b)\big) - c^-\big(\Gamma_1^{\uparrow}(b) + \Gamma_1^{\downarrow}(a)\big)\,. \tag{21}$$

3.4.3 Numerical scheme

Finally, we can write the following finite volume scheme: $\forall K \in \mathcal{T}_h$,

$$U_K^0 = \frac{1}{|K|}\int_K U_0(x)\,dx,\ W_K^0 = \frac{1}{|K|}\int_K W_0(x)\,dx, \tag{22}$$

$$V_K^0 = \frac{1}{|K|}\int_K V_0(x)\,dx, \forall K \in \mathcal{T}_h\,.$$

Then, for all $n \in \{1,\cdots,\tilde{N}\}$,

$$|K|\frac{U_K^{n+1}-U_K^n}{\Delta t} - \sum_{L\in N(K)} \tau_{K,L}^q (A(U_L^{n+1}) - A(U_K^{n+1})) + \sum_{L\in N(K)} G(U_K^{n+1}, U_L^{n+1}; \delta V_{K,L}^{n+1}) = \mu_1 |K| U_K^{n+1}(1 - U_K^{n+1} - \alpha_1 W_K^n)\,, \tag{23}$$

$$|K|\frac{W_K^{n+1}-W_K^n}{\Delta t} - \sum_{L\in N(K)} \tau_{K,L}^r (B(W_L^{n+1}) - B(W_K^{n+1})) + \sum_{L\in N(K)} G(W_K^{n+1}, W_L^{n+1}; \delta V_{K,L}^{n+1}) = \mu_2 |K| W_K^{n+1}(1 - W_K^{n+1} - \alpha_2 U_K^n)\,, \tag{24}$$

$$|K|\frac{V_K^{n+1}-V_K^n}{\Delta t} - \sum_{L\in N(K)} \tau_{K,L}^s (V_L^{n+1} - V_K^{n+1}) = -|K|(\alpha U_K^n + \beta W_K^n) V_K^{n+1}\,. \tag{25}$$

The discrete solution of the scheme (23)-(25) is a triplet (U_h, W_h, V_h) of piecewise constant functions on Q_T given by:

$$\forall K \in \mathcal{T}_h,\ \forall n \in \{0,\cdots,\tilde{N}-1\},\ U_h|_{]t^n,t^{n+1}]\times K} = U_K^{n+1},$$

$$W_h|_{]t^n,t^{n+1}]\times K} = W_K^{n+1},\ V_h|_{]t^n,t^{n+1}]\times K} = V_K^{n+1}\,.$$

4 Convergence of the numerical scheme

This section focuses on the study of the convergence of the generalized Finite Volume scheme introduced in the previous section. We will begin by stating the convergence theorem followed by its proof, which involves constructing a priori estimates and using compactness arguments.

Theorem 4.1 (Convergence of the scheme)**.** *Under the assumptions* (6), (8) *and* (9),
1) There exists a solution (U_h, W_h, V_h) *of the discrete system* (23)-(25) *with the initial condition*(22).
2) Any sequence $(h_{\tilde{m}})_m$ *that tends to* 0 *has a subsequence such that* $(U_{h_{\tilde{m}}}, W_{h_{\tilde{m}}}, V_{h_{\tilde{m}}})$ *converges a.e. in* Q_T *to a weak solution* (U, W, V) *of the system* (3)-(5) *in the sense of Definition 2.1.*

The proof of this Theorem is detailed in the following subsections.

4.1 A priori Analysis

4.1.1 Discrete Maximum Principle

Lemma 4.2. *Let* $(U_K^{n+1}, W_K^{n+1}, V_K^{n+1})_{K\in\mathcal{T}_h,\, n\in\{0,\cdots,\tilde{N}\}}$ *be the discrete solution of the scheme* (23)-(25). *Then, for all* $K \in \mathcal{T}_h$ *and for all* $n \in \{0,\cdots,\tilde{N}\}$, *we have:* $0 \le U_K^{n+1} \le 1$, $0 \le W_K^{n+1} \le 1$ *and* $V_K^{n+1} \ge 0$.

Proof: We proceed by induction on n. Thanks to the initial assumption (9), this statement is true for $n = 0$. Assume it holds for step n and let's show by contradiction that it remains true for step $n+1$ ($U_K^{n+1} \ge 0$). Suppose $U_K^{n+1} < 0$ and that $U_K^n \ge 0$. Consider a fixed volume K such that $U_K^{n+1} = \min\{U_L^{n+1}\}_{L\in\mathcal{T}_h}$. Multiply the equation (23) by -$(U_K^{n+1})^-$, then we get:

$$-|K|\frac{U_K^{n+1}-U_K^n}{\Delta t}(U_K^{n+1})^- + \sum_{L\in N(K)} \tau_{K,L}^q\big(A(U_L^{n+1}) - A(U_K^{n+1})\big)(U_K^{n+1})^- - \sum_{L\in N(K)} G(U_K^{n+1}, U_L^{n+1}; \delta V_{K,L}^{n+1})(U_K^{n+1})^- = -\mu_1 U_K^{n+1}(1-U_K^{n+1})(U_K^{n+1})^- - \mu_1\alpha_1 W_K^n (U_K^{n+1})^-\,.$$

Therefore, the extension of Γ_1 by 0 outside $[0,1]$ imply that

$$G(U_K^{n+1}, U_L^{n+1}; \delta V_{K,L}^{n+1}) \le G(U_K^{n+1}, U_K^{n+1}; \delta V_{K,L}^{n+1})$$

$$= \delta V_{K,L}^{n+1}\, \Gamma_1(U_K^{n+1}) = 0\,.$$

The monotonicity of the operator A, the hypothesis of induction and the positivity of transmissivities $\tau_{K,L}$ imply that

$$-|K|\frac{U_K^{n+1}-U_K^n}{\Delta t}(U_K^{n+1})^- \leq 0\,.$$

This inequality is satisfied if $(U_K^{n+1})^- = \min\{-U_K^{n+1}, 0\} \leq 0$, which leads to a contradiction.

By following a similar reasoning, we can show that $U_K^{n+1} \leq 1$ by multiplying (23) by $(U_K^{n+1}-1)^+$ and the proof is achieved easily.

4.1.2 Discrete A priori estimates

Under the assumption of positive transmissivities, the following a priori estimates are detailed in Proposition 3.2 of [33].

Proposition 4.3. *Let $(U_K^{n+1}, W_K^{n+1}, V_K^{n+1})_{K\in\mathcal{T}_h,\, n\in\{0,\cdots,\tilde{N}-1\}}$ be the discrete solution of the problem (23)-(25). Then, there exists a constant M depending on $||V_0||_\infty$, α, β and T such that:*

$$V_K^n \leq M\,. \tag{26}$$

Furthermore, there exists a constant $\tilde{C} > 0$ depending on Ω, T, $||V_0||_\infty$, α and d such that:

$$\frac{1}{2}\sum_{n=0}^{\tilde{N}-1}\Delta t \sum_{K\in\mathcal{T}_h}\sum_{L\in N(K)}\tau_{K,L}^q\Big|A(U_K^{n+1})-A(U_L^{n+1})\Big|^2 \tag{27}$$

$$+\frac{1}{2}\sum_{n=0}^{\tilde{N}-1}\Delta t \sum_{K\in\mathcal{T}_h}\sum_{L\in N(K)}\tau_{K,L}^r\Big|B(W_K^{n+1})-B(W_L^{n+1})\Big|^2$$

$$+\frac{1}{2}\sum_{n=0}^{\tilde{N}-1}\Delta t \sum_{K\in\mathcal{T}_h}\sum_{L\in N(K)}\tau_{K,L}^s\Big|V_K^{n+1}-V_L^{n+1}\Big|^2 \leq \tilde{C}\,.$$

4.2 Existence of a discrete solution

Proposition 4.4. *The problem (23)-(25) admits at least one solution $(U_K^{n+1}, W_K^{n+1}, V_K^{n+1})_{K\in\mathcal{T}_h,\, n\in\{0,\cdots,\tilde{N}-1\}}$.*

Proof: We demonstrate the existence of a discrete solution by induction on n. Assume that (U_h^n, W_h^n, V_h^n) exists, and we aim to show the existence of $(U_h^{n+1}, W_h^{n+1}, V_h^{n+1})$.

Equation (25) is a finite volume discretization of a linear parabolic equation, implicit in time. It forms a finite-dimensional linear system concerning the unknowns $\{V_K^{n+1}, K \in \mathcal{T}_h\}$. Therefore, we only need to show by induction that the unique solution to the associated homogeneous system is zero ($AV = 0 \Rightarrow V = 0$), from which the existence and uniqueness of V_h^{n+1} follow. Indeed, suppose $g = 0$ and $V_K^n = 0$, we then show that $V_K^{n+1} = 0$ for all $K \in \mathcal{T}_h$. Multiplying the associated homogeneous discrete equation (25) by V_K^{n+1} and summing over all volumes $K \in \mathcal{T}_h$, we obtain:

$$\sum_{K\in\mathcal{T}_h}|K|(V_K^{n+1})^2+$$

$$\sum_{K\in\mathcal{T}_h}\sum_{L\in N(K)}\mu_{K,L}^s(V_L^{n+1}-V_K^{n+1})^2$$

$$+\alpha\sum_{K\in\mathcal{T}_h}|K|U_K^n(V_K^{n+1})^2+\beta\sum_{K\in\mathcal{T}_h}|K|W_K^n(V_K^{n+1})^2 = 0.$$

It follows that $||V_h^{n+1}||_{L^2(\Omega)}^2 = 0$ and that $V_K^{n+1} = 0$ for all $K \in \mathcal{T}_h$.

Next, we can rewrite equation (23) in terms of p_h^i with $U_h^i = A^{-1}(P_h^i)$; $i \in \{0,\cdots,\tilde{N}-1\}$. Suppose that P_h^n and V_h^{n+1} exist. We introduce the scalar product $[.,.]$ on $\mathbb{R}^{\mathcal{T}_h}$ and we define the mapping $\mathcal{M}$, which associates to a vector $\mathcal{P} = (P_K^{n+1})_{K\in\mathcal{T}_h}$ the following expression, derived from equation (23):

$$\mathcal{M}(\mathcal{P}) = \Big(|K|\frac{A^{-1}(P_K^{n+1})-A^{-1}(P_K^n)}{\Delta t}$$

$$-\sum_{L\in N(K)}\tau_{K,L}^q(P_L^{n+1}-P_K^{n+1})$$

$$+\sum_{L\in N(K)}G(A^{-1}(P_K^{n+1}),A^{-1}(P_L^{n+1});\delta V_{K,L}^{n+1})$$

$$-\mu_1|K|P_K^{n+1}(1-P_K^{n+1}-\alpha_1 W_K^n)\Big)_{K\in\mathcal{T}_h}\,.$$

Multiplying by P_K^{n+1}, summing over all volumes $K \in \mathcal{T}_h$ and using estimates (26), (27) and Young's inequality, we deduce that:

$$[\mathcal{M}(\mathcal{P}),\mathcal{P}] \geq C|\mathcal{P}|^2 - C'|\mathcal{P}| - C'' \geq 0$$

$$\text{for } |\mathcal{P}| \text{ sufficiently large ,}$$

where C, C' and C'' are strictly positive constants. Consequently,

$$[\mathcal{M}(\mathcal{P}),\mathcal{P}] > 0 \text{ for } |\mathcal{P}| \text{ sufficiently large.}$$

This implies that there exists a vector $\mathcal{P}$ such that

$$\mathcal{M}(\mathcal{P}) = 0\,.$$

To demonstrate this, assume by contradiction that no $\mathcal{P}$ satisfies $\mathcal{M}(\mathcal{P}) = 0$. In that case, on a ball centered at O with radius k, we can define the following mapping:

$$\begin{array}{rcccl} S & : & \bar{B}(0,k) & \to & \bar{B}(0,k) \\ & & \mathcal{P} & \mapsto & S(\mathcal{P}) = -\frac{k\mathcal{M}(\mathcal{P})}{[\mathcal{M}(\mathcal{P})]}. \end{array}$$

The map S is continuous due to the continuity of $\mathcal{M}$ and the norm $[\mathcal{M}(\mathcal{P})]$ is nonzero on the convex and compact ball $\bar{B}(0,R)$. By Brouwer's fixed-point theorem, there exists $\mathcal{W}$ such that

$$-\frac{k\mathcal{M}(\mathcal{P})}{[\mathcal{M}(\mathcal{P})]} = \mathcal{P}\,. \tag{28}$$

Taking the norm on both sides of this equation, we get $[\mathcal{P}] = k > 0$, and taking the scalar product with $\mathcal{P}$ on both sides of (28) gives $[\mathcal{P},\mathcal{P}] = [\mathcal{P}]^2 = -k\frac{[\mathcal{M}(\mathcal{P}),\mathcal{P}]}{[\mathcal{P}]} \leq 0$ which is a contradiction. Therefore, P_h^{n+1} exists and hence U_h^{n+1} exists.

4.3 Compactness Estimates on Discrete Solutions

We now present estimates for the time and space translations of the discrete function w_h with $w_h = A(U_h)$, $B(W_h)$ or V_h, necessary for applying compactness arguments.

Lemma 4.5. *There exists a constant $C(\Omega,\ T,\ U_0,\ W_0,\ V_0) > 0$ such that:*

$$\iint_{\Omega'\times[0,T]} \left|w_h(t,x+\xi) - w_h(t,x)\right|^2 dxdt \tag{29}$$

$$\leq C|\xi|(|\xi|+2h),\ \forall \xi \in \mathbb{R}^d$$

with $\Omega' = \{x \in \Omega,\ [x,x+\xi] \subset \Omega\}$ and

$$\iint_{\Omega\times[0,T-\tau]} \left|w_h(t+\tau,x) - w_h(t,x)\right|^2 dxdt \tag{30}$$

$$\leq C(\tau+\Delta t),\ \forall \tau \in [0,T]\,.$$

Proof: First, we simplify the notation by writing:

$$\sum_{\sigma_{K,L}} \text{ instead of } \sum_{[(K,L)\in\mathcal{T}_h^2,\, K\neq L,\, |\sigma_{K,L}|\neq 0]}\,.$$

Let $\xi \in \mathbb{R}^3$ and $L \in N(K)$. We define the following function on Ω':

$$\beta_{\sigma_{K,L}}(x) = \begin{cases} 1 & \text{if } [x,x+\xi] \text{ intersects } \sigma_{K,L} \\ 0 & \text{otherwise} \end{cases}\,.$$

Next, define $c_{\sigma_{K,L}} = \left|\frac{\xi}{|\xi|}\cdot\eta_{K,L}\right|$, and observe

$$\text{i)}\ \int_{\Omega'} \beta_{\sigma_{K,L}}(x)\,dx \leq |\sigma_{K,L}|\big|\xi\big|c_{\sigma_{K,L}}\,,$$

because $\int_{\Omega'} \beta_{\sigma_{K,L}}(x)dx$ is the measure of the set of points in Ω' that are located inside a cylinder with base $\sigma_{K,L}$ and generator vector $-\xi$. Additionally,

$$\text{ii)}\ \sum_{\sigma_{K,L}} \beta_{\sigma_{K,L}}(x)c_{\sigma_{K,L}}d_{K,L} \leq |\xi| + 2h\,.$$

Indeed, since Ω is not necessarily convex, it is possible that $[x,x+\xi] \not\subset \bar{\Omega}$. To avoid this, let y' and $z' \in [x,x+\xi]$, where $y' \neq z'$ and the segment $[y',z'] \subset \bar{\Omega}$. There exist two volumes K and $L \in \mathcal{T}_h$ such that: $y' \in \bar{K}$ and $z' \in \bar{L}$. Thus,

$$\sum_{\sigma_{K,L}} \beta_{\sigma_{K,L}}(x)c_{\sigma_{K,L}}d_{K,L} = \left|(y_1 - z_1)\cdot\frac{\xi}{|\xi|}\right|,$$

where $y_1 = x_K$ or x_σ with $\sigma \in \mathcal{E}_{ext} \cap \mathcal{E}_K$ and $z_1 = x_L$ or $x_{\sigma'}$ with $\sigma' \in \mathcal{E}_{ext} \cap \mathcal{E}_L$ depending on the position of y' and z' in $\bar{K}$ or $\bar{L}$ respectively. Given that $y_1 = y' + y_2$ with $|y_2| \leq h$ and $z_1 = z' + z_2$ with $|z_2| \leq h$, we have

$$\left|(y_1 - z_1).\frac{\xi}{|\xi|}\right| \leq |y'-z'| + |y_2| + |z_2| \leq |\xi| + 2h\,.$$

Moreover, using the Cauchy-Schwarz inequality and estimate (27), we obtain:

$$I = \iint_{\Omega'\times[0,T]} \left|A(U_h)(t,x+y) - A(U_h)(t,x)\right|^2 dxdt$$

$$\leq \iint_{\Omega'\times[0,T]} \Big(\sum_{\sigma_{K,L}} |A(U_L^{n+1}) - A(U_K^{n+1})|\beta_{\sigma_{K,L}}(x)\Big)^2\,.$$

Next, we multiply and we divide by $d_{K,L}c_{\sigma_{K,L}}$. Therefore,

$$I \leq (T\sum_{\sigma_{K,L}} \beta_{\sigma_{K,L}}(x)d_{K,L}c_{\sigma_{K,L}}) \sum_{n=0}^{\tilde{N}-1}$$

$$\Delta t \sum_{\sigma_{K,L}} \frac{|A(U_L^{n+1}) - A(U_K^{n+1})|^2}{d_{K,L}c_{\sigma_{K,L}}} \int_{\Omega'} \beta_{\sigma_{K,L}}(x))\,dx$$

$$\leq CT|y|(|y|+2h)\,.$$

Otherwise, the time translation estimate (30) can be derived using classical techniques and hence the proof of the Lemma is completed.

4.4 Passing to the limit

In this section, we show the convergence of the discrete solution towards a limit, which is the weak solution of the continuous problem in the sense of Definition 2.1.

Lemma 4.6. *There exists a sequence* $(h_{\tilde{m}})_{\tilde{m}\in\mathbb{N}}$ *such that* $h_{\tilde{m}} \to 0$ *as* $\tilde{m} \to \infty$ *and triplets* (U, W, V) *over* Q_T *satisfying* $0 \leq M \leq 1$, $A(U)$, $B(W)$ *and* $V \in L^2(0,T;H^1(\Omega))$, *such that:*

$$i)\, U_{h_{\tilde{m}}} \to U,\ W_{h_{\tilde{m}}} \to W \text{ and } V_{h_{\tilde{m}}} \to V \quad (31)$$

$$\text{a.e. in } Q_T \text{ and strongly in } L^p(Q_T);\ 1 \leq p < +\infty\,,$$

$$ii)\, \nabla_{h_{\tilde{m}}} A(U_{h_{\tilde{m}}}) \rightharpoonup \nabla A(U),\ \nabla_{h_{\tilde{m}}} B(W_{h_{\tilde{m}}}) \rightharpoonup \nabla B(W) \quad (32)$$

$$\text{and } \nabla_{h_{\tilde{m}}} V_{h_{\tilde{m}}} \rightharpoonup \nabla V \text{ in } (L^2(Q_T))^d\,,$$

$$iii)\, q_h(x) \to q(x) \text{ a.e. in } \Omega\,. \quad (33)$$

Proof: The Lemma 4.5 and Kolmogorov compactness criteria imply the existence of a subsequence of U_h such that:

$$A(U_h) \longrightarrow \bar{A} \text{ in } L^2(Q_T)\,.$$

The operator A is strictly monotone. This leads to a unique density U such that $A(U) = \bar{A}$. Therefore,

$$A(U_h) \longrightarrow A(U) \text{ in } L^2(Q_T) \text{ and a.e. in } Q_T\,. \quad (34)$$

As we have A^{-1} is well-defined and continuous, we apply the norm L^∞ to U_h and the Lebesgue dominated convergence Theorem to $U_h = A^{-1}(A(U_h))$, we have: $\forall 1 \leq \text{ p } < +\infty$,

$$U_h \longrightarrow U \text{ in } L^p(Q_T) \text{ and a.e. in } Q_T\,.$$

Following similar guidelines, the time and the space translation estimates and the boundedness in $L^\infty$of V_h in (26) lead to the extraction of a subsequence V_h such that: $\forall 1 \leq \text{ p } < +\infty$,

$$V_h \longrightarrow V \text{ in } L^p(Q_T) \text{ and a.e. in } Q_T\,.$$

Let us now prove (32). Due to the estimate (27), we have $\nabla_{h_{\tilde{m}}} A(U_{h_{\tilde{m}}}) \rightharpoonup \Gamma$ in $L^2(Q_T)$. It remains to prove that $\Gamma = \nabla A(U)$ in the following steps:

Step 1: Prove that:

$$E_{h_{\tilde{m}}} = \iint_{Q_T} \nabla_{h_{\tilde{m}}} A(U_{h_{\tilde{m}}})\varphi\, dxdt + \iint_{Q_T} A(U_{h_{\tilde{m}}})\nabla\cdot\varphi\, dxdt \overset{h_{\tilde{m}}\to 0}{\longrightarrow} 0\,.$$

One has:

$$\int_\Omega A(U_{h_{\tilde{m}}})(x,t)\nabla\cdot(\varphi(x,t))\, dx$$

$$= \sum_{K\in\mathcal{T}_h} \int_K A(U_{h_{\tilde{m}}})(x,t)\nabla\cdot(\varphi(x,t))\, dx$$

$$= \sum_{K\in\mathcal{T}_h} \sum_{L\in N(K)} A(U_K^{n+1}) \int_{\sigma_{K,L}} \varphi(s,t)\eta_{K,L}\, ds$$

$$= \frac{1}{2} \sum_{K\in\mathcal{T}_h} \sum_{L\in N(K)} (A(U_K^{n+1}) - A(U_L^{n+1})) \int_{\sigma_{K,L}} \varphi(s,t)\eta_{K,L}\, ds\,.$$

Using the Definition (13) of the discrete gradient, we have:

$$\int_\Omega \nabla_{h_{\tilde{m}}} A(U_{h_{\tilde{m}}})\varphi\, dx =$$

$$\frac{1}{2} \sum_{K\in\mathcal{T}_h} \sum_{L\in N(K)} \int_{T_{K,L}} \nabla_{h_{\tilde{m}}} A(U_{h_{\tilde{m}}})\varphi\, dx$$

$$= -\frac{1}{2} \sum_{K\in\mathcal{T}_h} \sum_{L\in N(K)} (A(U_K^{n+1}) - A(U_L^{n+1})) \frac{|\sigma_{K,L}|}{|T_{K,L}|} \int_{T_{K,L}} \varphi(x,t)\eta_{K,L}\, dx\,.$$

The smoothness of φ and the Taylor formula imply that:

$$\Big|\frac{1}{|T_{K,L}|}\int_{T_{K,L}} \varphi(x,t)\eta_{K,L}\, dx - \frac{1}{|\sigma_{K,L}|}\int_{\sigma_{K,L}} \varphi(s,t)\eta_{K,L}\, ds\Big| \leq h_{\tilde{m}}||\varphi||_{C^1(\overline{\Omega_T})}\,.$$

Using Cauchy-Schwarz inequality and estimate (27):

$$2|E_{h_{\tilde{m}}}| \leq h_{\tilde{m}}||\varphi||_{C^1(\overline{\Omega_T})}$$

$$\sum_{n=0}^{\tilde{N}-1} \Delta t \sum_{K\in\mathcal{T}_h} \sum_{L\in N(K)} \big|A(U_L^{n+1}) - A(U_K^{n+1})\big||\sigma_{K,L}|$$

$$\leq h_{\tilde{m}}\sqrt{C}||\varphi||_{C^1(\overline{\Omega_T})}\Big(\sum_{n=0}^{\tilde{N}-1} \Delta t \sum_{K\in\mathcal{T}_h} \sum_{L\in N(K)} d_{K,L}|\sigma_{K,L}|\Big)^{\frac{1}{2}}\,.$$

Next, recall the orthogonality condition in admissible meshes, which implies that:

$$d_{K,L}|\sigma_{K,L}| = d|T_{K,L}|\,, \quad (35)$$

and that:

$$\sum_{K\in\mathcal{T}_h}\sum_{L\in N(K)}|T_{K,L}| = 2|\Omega|\,.$$

Consequently,

$$E_{h_{\tilde{m}}} \leq \frac{1}{2}h_{\tilde{m}}||\varphi||_{C^1(\overline{\Omega_T})}\sqrt{2CTd|\Omega|}\overset{h_{\tilde{m}}\to 0}{\longrightarrow} 0\,.$$

Step 2:
The fisrt step and assertion (34) imply that:

$$(\nabla_{h_{\tilde{m}}}A(U_{h_{\tilde{m}}}),\,\varphi)\to -(A(U_{h_{\tilde{m}}}),\,\nabla\cdot\varphi)$$
$$\to -(A(U),\,\nabla\cdot\varphi)\to(\nabla A(U),\,\varphi)\,.$$

Otherwise, the weak convergence in $L^2(Q_T)$ from (27) gives:

$$(\nabla_{h_{\tilde{m}}}A(U_{h_{\tilde{m}}}),\,\varphi)\to(\Gamma,\,\varphi)\,.$$

Therefore, $\Gamma = \nabla A(U)$.

Finally, we prove (33) using the approximation q_h defined in (19). $\forall q\in L^\infty(\Omega)\subset L^1(\Omega)$, we recall that the constant function on each diamond $T_{K,L}$ is defined as:

$$q_h(x) = \frac{1}{|T_{K,L}|}\int_{T_{K,L}} q(x)\,dx\,.$$

For $\varphi\in C^0(\Omega)$, we have $\Pi_h\varphi(x) = \frac{1}{|T_{K,L}|}\int_{T_{K,L}}\varphi(x)\,dx\to\varphi(x)$ a.e. and $|\Pi_h\varphi(x)|\leq ||\varphi||_{L^\infty(\Omega)}$. Applying the Lebesgue dominated convergence Theorem, we obtain $\Pi_h\varphi\to\varphi$ strongly in $L^1(\Omega)$. Moreover, the density implies

$$\forall q\in L^1(\Omega),\,\exists\varphi\in C^0(\Omega);\,||q-\varphi||_{L^1(\Omega)}\leq\varepsilon\,.$$

Therefore,

$$||q_h-q||_{L^1(\Omega)}\leq||q_h-\Pi_h\varphi||_{L^1(\Omega)}+||\Pi_h\varphi-\varphi||_{L^1(\Omega)}$$
$$+||q-\varphi||_{L^1(\Omega)}\overset{h\to 0}{\longrightarrow}0\,.$$

Thus, one can easily deduce (33).

Lemma 4.7. *The limit functions U, W and V constructed in Lemma 4.6 constitute a weak solution of the problem* (3)-(5) *in the sence of Definition 2.1.*

Proof: Let $\varphi_K^n := \varphi(t^n,x_K),\forall K\in\mathcal{T}_h$ and $n\in\{0,\cdots,\tilde{N}-1\}$ with $\varphi\in\mathcal{D}([0,T[\times\bar{\Omega})$. Multiply (23) by $\Delta t\varphi_K^{n+1}$ and add for all $K\in\mathcal{T}_h$ and $n\in\{0,\cdots,\tilde{N}-1\}$. One obtains:

$$S_1^h+S_2^h+S_3^h = 0\,,$$

where

$$S_1^h := \sum_{n=0}^{\tilde{N}-1}\Delta t\sum_{K\in\mathcal{T}_h}|K|(U_K^{n+1}-U_K^n)\varphi_K^{n+1}$$

$$S_2^h :=$$

$$-\sum_{n=0}^{\tilde{N}-1}\Delta t\sum_{K\in\mathcal{T}_h}\sum_{L\in N(K)}\tau_{K,L}^q(A(U_L^{n+1})-A(U_K^{n+1}))\varphi_K^{n+1}$$

$$S_3^h := \sum_{n=0}^{\tilde{N}-1}\Delta t\sum_{K\in\mathcal{T}_h}\sum_{L\in N(K)}G(U_K^{n+1},U_L^{n+1},\delta V_{K,L})\varphi_K^{n+1}$$

$$S_4^h := \mu_1\sum_{n=0}^{\tilde{N}-1}\Delta t\sum_{K\in\mathcal{T}_h}|K|U_K^{n+1}(1-U_K^{n+1}-\alpha_1W_K^n)\varphi_K^{n+1}\,.$$

Term of evolution in time . Using an integration by parts and taking $\varphi_K^{\tilde{N}}=0$ for all $K\in\mathcal{T}_h$ to obtain:

$$S_1^h = -\sum_{n=0}^{\tilde{N}-1}\sum_{K\in\mathcal{T}_h}|K|U_K^{n+1}(\varphi_K^{n+1}-\varphi_K^n)$$
$$-\sum_{K\in\mathcal{T}_h}|K|U_K^0\varphi_K^0$$
$$= -\sum_{n=0}^{\tilde{N}-1}\sum_{K\in\mathcal{T}_h}\int_{t^n}^{t^{n+1}}\int_K U_K^{n+1}\partial_t\varphi(t,x_K)\,dxdt$$
$$-\sum_{K\in\mathcal{T}_h}\int_K U_0(x)\varphi(0,x_K)\,dxdt$$
$$= -\int_0^T\int_\Omega U_h(t,x)\partial_t\varphi(t,x_K)\,dxdt$$
$$-\int_\Omega U_0(x)\varphi(0,x_K)dx\,.$$

We define

$$\tilde{S}_1^h = -\int_0^T\int_\Omega U\partial_t\varphi\,dxdt-\int_\Omega U_0\varphi(0,.)\,dx$$

Using the regularity of the test function φ, applying Taylor formula and using Lemma 4.6 i), we deduce that:

$$|S_1^h-\tilde{S}_1^h|\overset{h\to 0}{\longrightarrow}0\,.$$

Diffusive Term. Adding by edges and applying again Taylor, we have:

$$S_2^h = \frac{1}{2}\sum_{n=0}^{\tilde{N}-1}\Delta t\sum_{K\in\mathcal{T}_h}\sum_{L\in N(K)}q_{K,L}\frac{1}{d}|\sigma_{K,L}|d_{K,L}d$$

$$\frac{A(U_L^{n+1})-A(U_K^{n+1})}{d_{K,L}}\frac{\varphi_L^{n+1}-\varphi_K^{n+1}}{d_{K,L}}$$

$$=\frac{1}{2}\sum_{n=0}^{\tilde{N}-1}\Delta t\sum_{K\in\mathcal{T}_h}\sum_{L\in N(K)}q_{K,L}|T_{K,L}|$$

$$(\nabla_{K,L}A(U_h^{n+1})\cdot\eta_{K,L})(\nabla\varphi(t^{n+1},\bar{x}_{K,L})\cdot\eta_{K,L})\,,$$

where $\bar{x}_{K,L}$ is a point of the segment $[x_K,x_L]$ and $\eta_{K,L}=\frac{x_L-x_K}{d_{K,L}}$. Thus,

$$S_2^h=\frac{1}{2}\sum_{n=0}^{\tilde{N}-1}\Delta t\sum_{K\in\mathcal{T}_h}\sum_{L\in N(K)}q_{K,L}|T_{K,L}|$$

$$\big(\nabla_{K,L}A(U_h^{n+1})\cdot\nabla\varphi(t^{n+1},\bar{x}_{K,L})\big)$$

$$=\int_0^T\int_\Omega q_h(x)\nabla_h A(U_h)\cdot(\nabla\varphi)_h\,dxdt\,,$$

where,

$$(\nabla\varphi)_h|_{]t^n,t^{n+1}]\times T_{K,L}}:=\nabla\varphi(t^{n+1},\bar{x}_{K,L})\,.$$

Then, it is clear from the Lemma 4.6 ii) and iii), the continuity of φ implying that $(\nabla\varphi)_h\to\nabla\varphi$ in $L^\infty(Q_T)$ and the Lebesgue dominated convergence theorem imply that:

$$\lim_{m\to+\infty}S_2^{h_{\tilde{m}}}=\int_0^T\int_\Omega q(x)\nabla A(U)\cdot\nabla\varphi\,dxdt\,.$$

Convective Term. Adding through edges implies

$$S_3^h:=-\frac{1}{2}\sum_{n=0}^{\tilde{N}-1}\Delta t\sum_{K\in\mathcal{T}_h}\sum_{L\in N(K)}G(U_K^{n+1},U_L^{n+1},\delta V_{K,L}^{n+1})$$

$$(\varphi_L^{n+1}-\varphi_K^{n+1})\,.$$

For each pair K and L of neighboring volumes, we introduce $U_{K,L}^{n+1}$ as the minimum of U_K^{n+1} and U_L^{n+1}. Then, we consider:

$$S_3^{h,*}:=-\frac{1}{2}\sum_{n=0}^{\tilde{N}-1}\Delta t\sum_{K\in\mathcal{T}_h}\sum_{L\in N(K)}\Gamma_1(U_{K,L}^{n+1})\delta V_{K,L}^{n+1}$$

$$(\varphi_L^{n+1}-\varphi_K^{n+1})\,.$$

Next, we introduce the following functions:

$$\overline{U_h}|_{]t^n,t^{n+1}]\times T_{K,L}}:=\max\{U_K^{n+1},U_L^{n+1}\},$$

$$\underline{U_h}|_{]t^n,t^{n+1}]\times T_{K,L}}:=\min\{U_K^{n+1},U_L^{n+1}\}\,.$$

According to the Definition of ∇_h and $(\nabla\varphi)_h$, we can write:

$$S_3^{h,*}:=-\frac{d}{2}\int_0^T\int_\Omega q_h(x)\Gamma_1(\underline{U_h})\nabla_h V_h\cdot(\nabla\varphi)_h\,dxdt\,.$$

Using the monotonicity of the operator A and the estimate (27), one has:

$$\int_0^T\int_\Omega\big|A(\overline{U_h})-A(\underline{U_h})\big|^2\le\sum_{n=0}^{\tilde{N}-1}\Delta t\sum_{K\in\mathcal{T}_h}\sum_{L\in N(K)}|T_{K,L}|$$

$$\big|A(U_L^{n+1})-A(U_K^{n+1})\big|^2$$

$$\le h^2\sum_{n=0}^{\tilde{N}-1}\Delta t\sum_{K\in\mathcal{T}_h}\sum_{L\in N(K)}\frac{|\sigma_{K,L}|}{d_{K,L}}|A(U_L^{n+1})-A(U_K^{n+1})|^2$$

$$\le Ch^2\,.$$

Therefore,

$$A(\overline{U_{h_{\tilde{m}}}})\to A(\underline{U_{h_{\tilde{m}}}})\text{ a.e. in }Q_T\text{ as }h_{\tilde{m}}\to 0\,.$$

The continuity of A^{-1} implies that,

$$\overline{U_{h_{\tilde{m}}}}\to\underline{U_{h_{\tilde{m}}}}\text{ a.e. in }Q_T\text{ as }h_{\tilde{m}}\to 0\,.$$

Then, Lemma 4.6 i), iii) and that $\underline{U_{h_{\tilde{m}}}}\le U_{h_{\tilde{m}}}\le\overline{U_{h_{\tilde{m}}}}$, lead to:

$$\Gamma_1(\underline{U_{h_{\tilde{m}}}})\to\Gamma_1(U)\text{ a.e. in }Q_T\text{ and in }L^p(Q_T),\ p<\infty\,.$$

The Lemma 4.6 ii) implies that

$$\lim_{m\to+\infty}S_3^{h_{\tilde{m}},*}=-\int_0^T\int_\Omega q(x)\Gamma_1(U)\nabla V\cdot\nabla\varphi\,dxdt\,.$$

It follows from the properties of G that:

$$|G(U_K^{n+1},U_L^{n+1},\delta V_{K,L}^{n+1})-\Gamma_1(U_{K,L}^{n+1})\delta V_{K,L}^{n+1}|$$

$$=|G(U_K^{n+1},U_L^{n+1},\delta V_{K,L}^{n+1})-G(U_{K,L}^{n+1},U_{K,L}^{n+1},\delta V_{K,L}^{n+1})|$$

$$\le|\delta V_{K,L}^{n+1}|w(d|U_L^{n+1}-U_K^{n+1}|)\,.$$

Hence,

$$|S_3^h-S_3^{h,*}|\le\int_0^T\int_\Omega q(x)w(2|\overline{U_h}-\underline{U_h}|)|\nabla_h V_h\cdot(\nabla\varphi)_h|\,.$$

Using Cauchy-Schwarz inequality, the uniform bound of $\nabla_h V_h$ from (27) and of q and the convergence $\overline{U_{h_{\tilde{m}}}}\to\underline{U_{h_{\tilde{m}}}}$, we deduce:

$$\lim_{m\to+\infty}S_3^{h_{\tilde{m}}}=-\int_0^T\int_\Omega q(x)\Gamma_1(U)\nabla V\cdot\nabla\varphi\,dxdt\,.$$

Additionally,

$$\lim_{m\to+\infty} S_4^{h_{\tilde{m}}} = \mu_1 \int_0^T \int_\Omega U(1-U-\alpha_1 W)\varphi \, dxdt\,.$$

Finally, we note that all convergence results may be applied to the second species W and the chemical concentration V using similar guidelines and reasoning methods.

5 Numerical Simulations

In this section, numerical experiments are conducted to enhance our theoretical results. These experiments are modeling the dynamics of two competing species under specific diffusion conditions and habitat heterogeneity. The discrete solutions are obtained using an extended Fortran 95 code for problems with heterogeneous and discontinuous diffusive coefficients. The computations were done according to the following algorithm: At each discrete time t_{n+1}, we first compute the solution V^{n+1} of the linear system defined by equation (25). Then, we calculate the solutions U^{n+1} (resp. W^{n+1}) of the nonlinear systems (23) (resp. (24)) using Newton's method to approximate the solution of the nonlinear system, along with a gradient method to solve the resulting linear systems from the Newton algorithm. To assess the effectiveness of the numerical method, we analyzed the convergence rates of the scheme under mesh refinement. By systematically decreasing the mesh size, the relative errors for all variables exhibit a clear trend of reduction, indicating that the method achieves consistent convergence toward the true solution. Moreover, the robustness of the method was tested by varying the heterogeneity and discontinuity of the diffusion coefficients. This robustness highlights the method's ability to handle challenging scenarios, including discontinuous diffusion and complex spatial domains, without sacrificing accuracy. Despite these variations, the numerical scheme maintained stability and produced accurate results across all test cases conducted on admissible meshes as in Figure 1.

5.1 Test 1: Exclusion with Habitat heterogeneity

In this test, we consider the full system (3) with the corresponding diffusive and convective coefficients. We suppose that $s = 1$ and we set $dt = 0.0005$, $\alpha = \beta = 1$, $\alpha_1 = 2$, $\alpha_2 = 0.1$, $\mu_1 = 0.8$, $\mu_2 = 0.6$ $a(U) = D_U U(1-U)$ with $D_U = 0.008$, $b(W) = D_W W(1-W)$ with $D_W = 0.2$, $\Gamma_1(U) = c_U U(1-U)$ with $c_U = 0.1$, $\Gamma_2(W) = c_W W(1-W)$ with $c = 0.1$. Moreover, the diffusive coefficient for the chemoattractant is $d = 5 \times 10^{-4}$.

Then, we take the parameters $L_x = 1$ and $L_y = 1$ representing the length and width of the Delaunay domain constructed using the Triangle software, as depicted in the right part of Figure 2. Next, the left part of Figure 2 shows that both species, with initial densities $U_0(x,y) = W_0(x,y) = 0.2$ are placed in a square $(x,y) \in \big([0.45, 0.55] \times [0.45, 0.55]\big)$, while the left part of Figure 3 depicts that the chemoattractant, with initial density $V_0(x,y) = 5$, is concentrated in four separate square regions $(x,y) \in \big([0.7, 0.8] \times [0.2, 0.3]\big) \cup \big([0.2, 0.3] \times [0.2, 0.3]\big) \cup \big([0.2, 0.3] \times [0.7, 0.8]\big) \cup \big([0.7, 0.8] \times [0.7, 0.8]\big)$. Subsequently, Figure 3 illustrates the dynamics of the chemical diffusion within these four regions.

Then, the system is tested under two main cases: The first case deals with $q = r = s = 1$ (homogeneous diffusion), and the second one deals with heterogeneous diffusion for species 1;

$$q(x,y) = \begin{cases} (x-0.5)^2 + (y-0.5)^2 & \text{if } y < 0.5 \\ 1 & \text{if } y \geq 0.5\,. \end{cases}$$

and a discontinuous oblique pipe diffusion for species 2,

$$r(x,y) = \begin{cases} 1 & \text{if } (x,y) \in \Omega_1 \cup \Omega_3 \\ 0.01 & \text{if } (x,y) \in \Omega_2\,, \end{cases}$$

in a unit square Ω divided into three subdomains:

$$\Omega_1 = \{(x,y) \in \Omega;\ \phi_1(x,y) < 0\},$$

$$\Omega_2 = \{(x,y) \in \Omega;\ \phi_1(x,y) > 0 \text{ and } \phi_2(x,y) < 0\},$$

$$\Omega_3 = \{(x,y) \in \Omega;\ \phi_2(x,y) > 0\},$$

where $\phi_1(x,y) = y + \delta(x-0.5) - 0.475$, $\phi_2(x,y) = \phi_1(x,y) - 0.05$ and the slope of the pipe is $\delta = 0.3$.

In the first case, Figure 4 highlights the dynamics of the competitive species spreading out uniformly across the domain. Hence, depending on how the chemicals influence them, they may cluster towards the chemoattractant regions. In the second case, Figure 5 and Figure 6 show the dynamics of the species separately while Figure 7 highlights the dynamics of the competitive species at the same time. One may remark that the diffusion of species 2 is based on the different regions of the domain divided by two lines ϕ_1 and ϕ_2, which create a pipe of slower diffusion. Due to the habitat complexity and the Lotka-Volterra competition with $\alpha_1 = 2$ and $\alpha_2 = 0.1$, one species might dominate certain

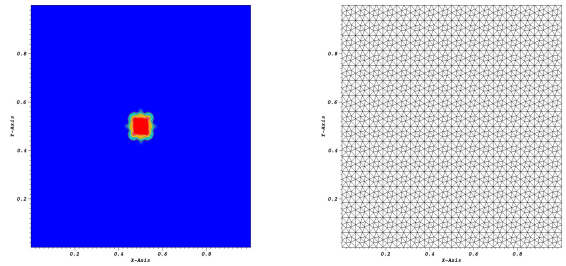

Figure 2: Initial density of species (a), Admissible mesh (b) .

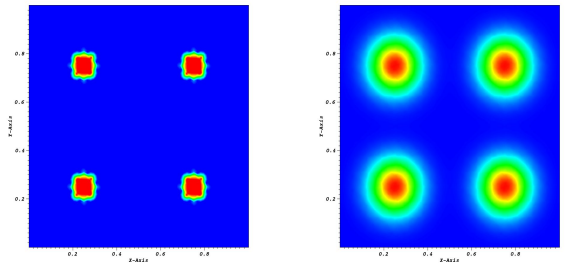

Figure 3: Initial density of the chemical (a), V-Evolution in time (b) .

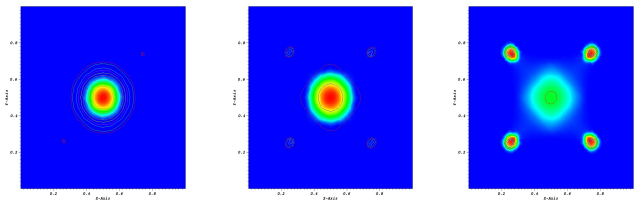

Figure 4: Evolution in time of species U and W.

regions while the other is excluded, leading to competitive exclusion. This explains why the density range of W decreases in Table (5), Table (6), and Table (7) while the density range of U increases. Moreover, the curves in Figure 8 will likely show how one species' density W decreases significantly over time, indicating exclusion.

Furthermore, the minimum, the maximum, and the relative errors for each component of the system are provided in Table (2), Table (3) and Table (4) for the first case and in Table (5), Table (6) and Table (7) for the second case. These tables capture the high accuracy of the numerical computations in terms of the average distribution and maximum pointwise for all variables in both cases. The smaller the relative errors, the more accurate the simulation is in predicting the distribution of the respective variables over the entire domain.

5.2 Test 2: Coexistence scenario

We consider the same Test 1 but with $\alpha_1 = \alpha_2 = 0.1$ and with random initial data for both species U and W. The closer α_1 and α_2 are closer to 0, the weaker the competition between species. Figure 9 and Figure 10 show that the environment supports a stable coexistence where both species can move without completely excluding each other. This coexistence case represents a balanced ecological scenario where neither species fully dominates, allowing for diverse spatial distributions across the domain.

6 Conclusion

This paper presents a generalized finite volume scheme to address and overcome all the challenges and difficulties arising from general nonlinear diffusive and convective coefficients. This method provides a robust framework for simulating the dynamics of species interactions and for capturing the essential behaviors even in cases with heterogeneity and discontinuities. The simulations demonstrated that the numerical approach can successfully capture the species' behavior in many scenarios of biological and ecological importance. This study may help to predict species coexistence, the evolution of drug resistance, patterns of infection spread, and the effectiveness of therapeutic interventions. Future work could expand on these findings by incorporating dynamic environments where the properties of the medium evolve over time and by extending the model to include multi-species interactions. Such advancements would enrich the understanding of chemotaxis-driven systems and offer valuable insights into ecological dynamics, bioengineering, and conservation planning.

Table 2: Case 1 at time $t = 0.015$

	U	W	V
Max	0.201	0.165	4.999
Min	0	0	0
Relative L^2-error	2.049×10^{-5}	7.235×10^{-5}	2.126×10^{-5}
Relative L^∞ error	4.526×10^{-3}	8.506×10^{-3}	4.611×10^{-3}

Table 3: Case 1 at time $t = 0.3$

	U	W	V
Max	0.203	0.041	4.808
Min	0	0	0
Relative L^2-**error**	1.436×10^{-7}	1.036×10^{-6}	1.260×10^{-7}
Relative L^∞ **error**	3.789×10^{-4}	1.018×10^{-3}	3.550×10^{-4}

Table 4: Case 1 at time $t = 2.5$

	U	W	V
Max	0.280	0.014	1.945
Min	0	0	0
Relative L^2-**error**	3.588×10^{-8}	1.044×10^{-7}	1.941×10^{-8}
Relative L^∞ **error**	1.894×10^{-4}	3.232×10^{-4}	1.393×10^{-4}

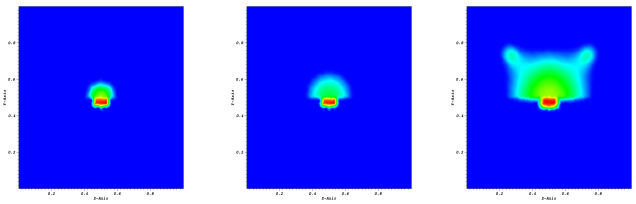

Figure 5: Evolution in time of species U .

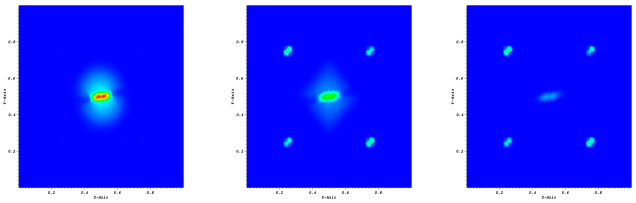

Figure 6: Evolution in time of species W .

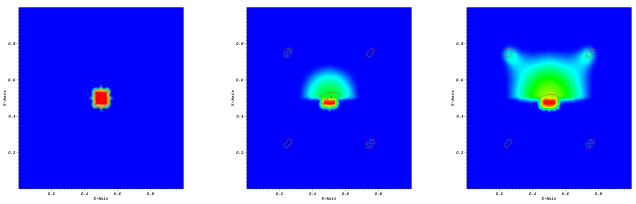

Figure 7: Evolution in time of both species .

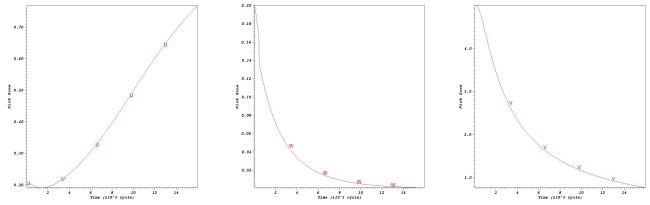

Figure 8: Time Evolution Curves of species U and W.

Table 5: Case 2 at time $t = 0.015$

	U	W	V
Max	0.205	0.194	4.998
Min	0	0	0
Relative L^2-**error**	2.137×10^{-5}	6.161×10^{-5}	2.182×10^{-5}
Relative L^∞ **error**	4.623×10^{-3}	7.850×10^{-3}	4.671×10^{-3}

Table 6: Case 2 at time $t = 0.3$

	U	W	V
Max	0.236	0.00063	4.709
Min	0	0	0
Relative L^2-**error**	1.164×10^{-7}	4.496×10^{-7}	1.352×10^{-7}
Relative L^∞ **error**	3.411×10^{-4}	6.705×10^{-3}	3.677×10^{-4}

Table 7: Case 2 at time $t = 2.5$

	U	W	V
Max	0.633	0.000043	2.005
Min	0	0	0
Relative L^2-**error**	2.027×10^{-8}	3.1951×10^{-8}	2.058×10^{-8}
Relative L^∞ **error**	1.424×10^{-4}	1.787×10^{-4}	1.435×10^{-4}

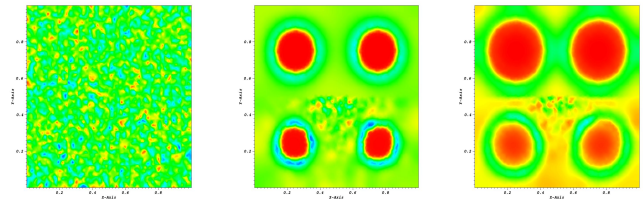

Figure 9: Evolution in time of species U .

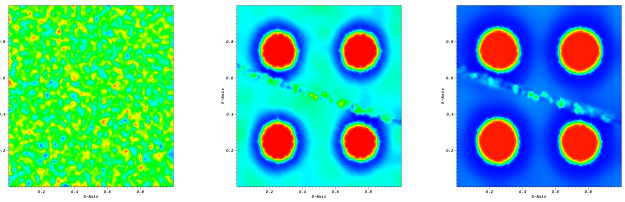

Figure 10: Evolution in time of species W.

References:

[1] E. F. Keller and L. A. Segel, *Model for chemotaxis.* Journal of theoretical biology, Vol. 30, No. 2, 1971, pp. 225-234.

[2] Z. Feng, J. Jia, and S. Zhou, *Stability of steady-state solutions of a class of Keller–Segel models with mixed boundary conditions.* Journal of Mathematical Methods in the Applied Sciences, Vol. 27, No. 12, 2024, pp. 9476-9492.

[3] Shen, J., Xu, J. *Fully decoupled and energy stable BDF schemes for a class of Keller-Segel equations.* J. Comput. Phys. Vol. 449, No. 110799, 2022.

[4] Wang, S., Zhou, S., Shi, S., Chen, W. *Unconditionally bound preserving and energy dissipative schemes for a class of Keller-Segel equations.* SIAM J. Numer. Anal. Vol. 58, No. 3, 2020, pp. 1674–1695.

[5] X. Huang and J. Shein, *Efficient Numerical Schemes for a Two-Species Keller-Segel Model and Investigation of Its Blowup Phenomena in 3D.* Acta Applicandae Mathematicae, Vol. 190, No. 1, 2024, DOI:10.1007/s10440-024-00647-0.

[6] Li, Y., Li, Y.X., *Finite-time blow-up in higher dimensional parabolic-parabolic Chemotaxis system for two species.* Nonlinear Anal., Theory Methods Appl. Vol. 109, 2014, pp. 72–84.

[7] D. Tran. T. Tran and V. Tran, *On the nonlocal parabolic-elliptic Keller-Segel model in bounded domains.* Communications on Pure and Applied Analysis, Vol. 23, No. 11, 2024, pp. 225-234.

[8] G. Chamoun, *Mathematical analysis of parabolic models with volume-filling effect in weighted networks.* Journal of Dynamics and Differential Equations, Vol. 35, No. 3, 2023, pp. 2115-2137.

[9] G. Chamoun, *An efficient numerical study for anisotropic nonlinear models of competitive swimming species.* WSEAS Transactions on Biology and Biomedicine, Vol 22, 2025, pp. 37-45.

[10] E. Rocca, G. Schimpera and A. Signori, *On a Cahn–Hilliard–Keller–Segel model with a generalized logistic source describing tumor growth.* Journal of Differential Equations, Vol 343, 2023, pp. 530-578.

[11] L. Shaikhet and A. Korobeinikov, *Persistence and Stochastic Extinction in a Lotka–Volterra Predator–Prey Stochastically Perturbed Model.* Mathematics, Vol. 12, No. 10, 2024, 1588, https://doi.org/10.3390/math12101588.

[12] S. Samir and Ferraro, Francesco and Grilletta, Christian and Azaele, Sandro and Maritan, Amos *Generalized Lotka-Volterra Systems with Time Correlated Stochastic Interactions.* Phys. Rev. Lett., Vol. 133, No. 16, 2024, pp. 167101-167107.

[13] A. J. Lotka, *Elements of physical biology.* Williams and Wilkins, 1925.

[14] V. Volterra, *Variations and fluctuations of the number of individuals in animal species living together.* ICES Journal of Marine Science, Vol. 3, No. 1, 1928, pp. 3-51.

[15] M. Di Francesco, A. Esposito, and S. Fagioli, *Nonlinear degenerate cross-diffusion systems with nonlocal interaction.* Nonlinear Anal., Vol. 169, 2018, pp. 94-117.

[16] T. Hillen and K. Painter, *Volume filling effect and quorum-sensing in models for chemosensitive movement.* Canadian App. Math., Vol. 10, 2002, pp. 501-543.

[17] G. Ren and B. Liu, *Global boundedness and asymptotic behavior in a two-species chemotaxis-competition system with two signals.* Nonlinear Anal. Real World Appl., Vol. 48, 2019, pp. 288-325.

[18] Q. Zhang, X. Liu, and X. Yang, *Global existence and asymptotic behavior of solutions to a two-species chemotaxis system with two chemicals.* J. Math. Phys., Vol. 58, No. 11, 2017, 111504.

[19] L.Wang, C. Mu, X. Hu, and P. Zheng, *Boundedness and asymptotic stability of solutions to a two-species chemotaxis system*

with consumption of chemoattractant. J. Differential Equations, Vol. 264, No. 5, 2018, pp. 3369-3401.

[20] G. Chamoun, M. Ibrahim, M. Saad and R. Talhouk, *Asymptotic behavior of solutions of a nonlinear degenerate chemotaxis model.* Discrete Syst. Ser. B, Vol. 25, 2020, pp. 4160-4188.

[21] Q. Al Farei and M. Boulbrachene *Mixing finite elements and finite differences in nonlinear Schwarz iterations for nonlinear elliptic PDEs.* Comp. Math. and Mod., Vol. 33, No. 1, 2022, pp. 77-94.

[22] F. Filbet, *A finite volume scheme for the Patlak-Keller-Segel chemotaxis model.* Numerische Mathematik, Vol. 104, No. 4, 2006, pp. 457-488.

[23] JI. Tello and M. Winkler, *Stabilization in a two-species chemotaxis system with a logistic source.* Nonlinearity, Vol. 25, No. 5, 2012, 1413.

[24] G. Zhou and N. Saito, *Finite volume methods for a Keller-Segel system: discrete energy, error estimates, and numerical blow-up analysis.* Numerische Mathematik, Vol. 135, No.1, 2017, pp. 265-311.

[25] S.M. Hassan and A.J. Harfash, *Finite Element Analysis of the Two-Competing-Species Keller-Segel Chemotaxis Model.* Comput Math Model, Vol. 33, 2022, pp. 443-471.

[26] J. A. Carrillo, F. Filbet, and M. Schmidtchen, *Convergence of a finite volume scheme for a system of interacting species with cross-diffusion.* Numer. Math., Vol. 145, No. 3, 2020, pp. 473-511.

[27] T. B. Issa, R. B. Salako, and W. Shen, *Traveling wave solutions for two species competitive chemotaxis systems.* 2020.

[28] J. I. Tello and D. Wrzosek, *Predator-prey model with diffusion and indirect prey-taxis.* Mathematical Models and Methods in Applied Sciences, Vol. 26, No. 11, 2016, pp. 2129-2162.

[29] C. Stinner, J.I. Tello and M. Winkler, *Competitive exclusion in a two-species chemotaxis model* J. Math Biol. , Vol. 68, No. 7, 2014, pp. 1607-1626.

[30] G. Li and Y. Yao, *Two-species competition model with chemotaxis: well-posedness, stability, and dynamics.* Nonlinearity, Vol 35, No. 3, 202, pp. 1329-1359.

[31] R. Bailo, J. A. Carrillo, and J. Hu., *Bound-preserving finite-volume schemes for systems of continuity equations with saturation.* SIAM J. Appl. Maths., Vol 83, No. 3, 2023, pp. 1315-1339.

[32] H.S. Alayachi, M. Abdelrahman, and K. Mohamed, *Finite-volume two-step scheme for solving the shear shallow water model.* SIAM J. Appl. Maths., Vol 9, No. 8, 2024, pp. 20118-20135.

[33] B. Andreianov, M. Bendahmane and M. Saad, *Finite volume methods for degenerate chemotaxis model.* Journal of Computational and Applied Mathematics, Vol., 235, 2011, pp. 4015-4031.

Contribution of Individual Authors to the Creation of a Scientific Article (Ghostwriting Policy)

The author contributed in the present research, at all stages from the formulation of the problem to the final findings and solution.

Sources of Funding for Research Presented in a Scientific Article or Scientific Article Itself

No funding was received for conducting this study.

Conflicts of Interest

The author has no conflicts of interest to declare.